MDPI

Article

An Empirical Study on the Friction of Reciprocating Rod Seals at Predefined Lubrication Conditions and Shear Rates

Oliver Feuchtmüller *[ID], Lothar Hörl and Frank Bauer [ID]

Institute of Machine Components, Faculty 7—Engineering Design, Production Engineering and Automobile Engineering, University of Stuttgart, 70569 Stuttgart, Germany; lothar.hoerl@ima.uni-stuttgart.de (L.H.); frank.bauer@ima.uni-stuttgart.de (F.B.)
* Correspondence: oliver.feuchtmueller@ima.uni-stuttgart.de

Abstract: A key factor influencing the friction of rod seals is a thin oil film, which is dragged into the sealing gap at outstroke and instroke. Accurate determination of oil film thickness in the sealing gap of rod seals is a challenging task since it is only in the range of a few nanometers. A novel measurement procedure to analyze the friction of common reciprocating sealing systems in direct relation to the shear rate and film thickness is introduced in this paper. Results from a first empirical study with film thicknesses in the range of a few nanometers and shear rates up to $\dot{\gamma} = 10^7 \text{ s}^{-1}$ were used to compare the friction of practically relevant polyurethane U-cups. The U-cups differ in their geometry and surface roughness. It is seen that even at such thin films, the measured friction of those seals can be approximated by Newtonian fluid friction (speed, film thickness, viscosity, contact area). In general, the novel measurement procedure is useful in a scientific and technical context, since it offers a new perspective on tribological mechanisms at thin film lubrication conditions.

Keywords: reciprocating rod seals; friction; thin film lubrication; film thickness measurements; high shear rates; empirical analysis

1. Introduction

Linear actuators such as hydraulic or pneumatic cylinders are used in a variety of applications. One critical component of every hydraulic or pneumatic cylinder is the rod seal; see Figure 1. If a rod seal fails, leakage or machine downtime is unavoidable. In high-precision positioning actuators, the rod seal's friction is of crucial importance, since it influences the dynamic performance and precision of the entire linear actuator. Consequently, the friction properties of rod seals should be considered when designing linear actuators. However, despite decades of research, predicting a seal's friction remains a challenging task due to numerous influencing parameters.
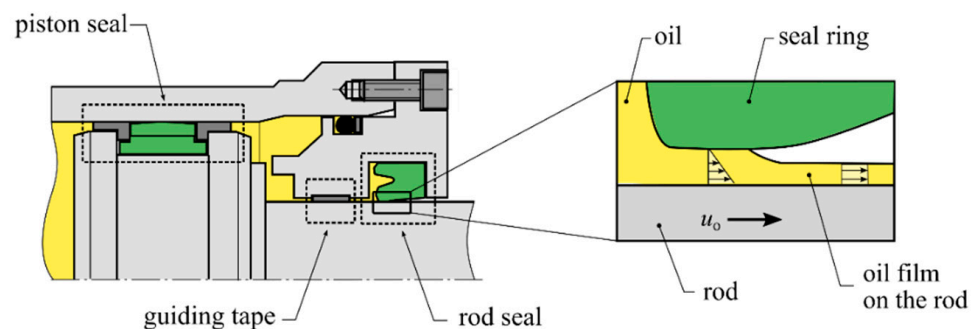

Figure 1. Schematic of a hydraulic cylinder (**left**) and the sealing gap of the rod seal at outstroke (**right**).

One key factor influencing the friction of rod seals is the oil film generation in the sealing gap [1,2]. At outstroke and instroke, the hydraulic rod drags oil into the sealing

gap, resulting in a thin lubricant film [1,3], see Figure 1. Depending on the film thickness in the sealing gap and the lubrication conditions, various tribological mechanisms may have an important influence on the friction. For example, at thin film lubrication, an increase in the apparent viscosity of lubricants caused by intermolecular forces between lubricants and counter surfaces was reported in tribological tests, e.g., [4–6]. An increase of viscosity in lubricated contacts increases the apparent shear and resulting friction. Further studies report a phenomenon called the wall slip, e.g., [7–11]. Wall slip is a relative motion between a lubricant's molecules and the counter surface and can occur due to poor wetting conditions and high shear. The influence of intermolecular forces between the components of the sealing system and phenomena such as wall slip cannot be ruled out. Furthermore, shear thinning of typical hydraulic oils was reported at high shear rates [12–14]. In conclusion, when friction phenomena of reciprocating rod seals are discussed, both the film thickness in the sealing gap and the shear rate should be known.

Numerous simulation models based on the so-called inverse theory of hydrodynamic lubrication (IHL) [15–18] and elastohydrodynamic lubrication (EHL) [19–21] have been developed. The accuracy of simulation models must be validated properly, preferably with comprehensive empirical data. In the narrow sealing gap of rod seals, even an absolute error of just few nanometers results in a great error of the expected shear rate and therefore in the calculated fluid friction. To predict the friction in elastohydrodynamic contacts, it is not sufficient to determine the film thickness and shear rate with precision. Moreover, the lubricants properties in such small gaps and high shear rates can significantly differ from their bulk properties [12–14]. Consequently, validated models for the rheological behavior of certain lubricants are required; see [22]. A further challenge arises when the counterfaces have a certain roughness and influence the shear flow in the gap [19,23,24]. In fact, all assumptions must be validated properly.

ISO 7986 [25] describes a standardized method and measuring apparatus to analyze the friction of rod seals. The method is very useful to compare different rod seals at certain operating conditions, such as rod speed, pressure, and temperature. A serious drawback of the standardized test rigs according to ISO 7986 [25] for analyzing the friction of rod seals is that the absolute film thickness in the sealing gap remains unknown. This limits conclusions which can be drawn on the actual tribological mechanisms in the sealing gap.

In general, the determination of the film thickness of rod seals is not trivial, e.g., [26]. Several empirical measurement methods have been developed over decades of research [27,28]. One challenge is that the film thickness of practical relevant rod seals, such as polyurethane U-cups, is only in the nanometer range [29,30]. Thus, highly accurate measurement devices are mandatory.

We developed a novel measurement procedure to analyze the influence of film thickness and shear rate on the friction of reciprocating rod seals. A test rig is used for measuring the friction at outstroke and an ellipsometer for film thickness measurements. One unique feature of the procedure is that a predefined lubricant film in the nanometer range is generated on the rod to achieve certain lubrication conditions and shear rates in the sealing gap. It is possible to determine the friction of various practical relevant seal rings and lubricants in direct relation to the fluid shear and thin film lubrication conditions. The procedure offers a deep insight into the influence of parameters such as the geometry and surface roughness of the seal ring and rheological properties of the lubricant on the friction. In a first empirical study, we compared the friction of three sealing rings which differ in their geometry and surface roughness.

2. Materials and Methods

For the empirical study, we used rod seals with different components; see Section 2.1. The new measurement procedure is based on a combination of film thickness measurements using an ellipsometer (see Section 2.2), and friction measurements using a new test rig (see Section 2.3). The main steps of the new measurement procedure are described in Section 2.4.

2.1. Components of the Analyzed Sealing Systems

The used sealing systems consist of three main components: the seal rings (U-cups), the lubricants (mineral oil), and the rod.

2.1.1. Seal Rings

Three different polyurethane U-cups were used as representative seal rings. The U-cups were manufactured by Freudenberg FST GmbH (Germany) and are suited for a rod diameter $d = 50$ mm. Further properties of the used U-cups are summarized in Figure 1. The U-cups differ in their profiles (cross-sections) named T20 and EW. A characteristic feature of the sealing rings with profile EW is a rounded sealing edge. In comparison, the T20 profile has a cut and sharp sealing edge, as is common for such seals. The seal rings with the profile EW were manufactured using two different molding tools. One tool was made using a lathing process in the area of the sealing edge and the other tool was eroded. The surfaces of the seals reflect the characteristic surface topographies of the molding tool cavities (lathed/smooth, eroded/rough). The material of the T20 and EW seal rings is a typical polyurethane with a Shore hardness of 95 ShA.

The radial loads of the three sealing rings were measured in advance using a device based on the split mandrel technique. Further information on the device is provided by Feldmeth [31] and can be found in the (withdrawn) standards [32,33]. Before the radial load was measured, each U-cup was stored for at least 24 h on a rod of nominal diameter ($d = 50$ mm) for relaxation purposes. According to recommendations by Feldmeth [31], the radial load of each U-cup was measured 10 s after pushing the U-cup over the split mandrel to obtain a representative value. The widths of the contact area between the rod and the sealing rings were measured after mounting the sealing rings on a hollow glass rod via a mirror using a digital microscope (Keyence VHX 3000). The radial loads of the rod seals and the widths of the contact between the rod and the seal rings are listed in Figure 2. The contact area

$$A = l_b \, d \, \pi \tag{1}$$

is the product of the contact width and the circumference of the rod.

Property	T20	EW-smooth	EW-rough
Geometry/Profile			
Sealing edge	sharp edge (cut)	round edge (moulded)	round edge (moulded)
Topography	150 µm	150 µm	150 µm
Radial load F_{rad}	531 N	542 N	536 N
Contact width l_b	0.91 mm	0.57 mm	0.57 mm

Figure 2. Properties of the three different U-cups analyzed in this study.

2.1.2. Hydraulic Oil

Various mineral oils without additives were used as lubricants. The oils are from a German research organization named "Forschungsvereinigung Antriebstechnik e.V." and supplied by Weber Reference Oils (Germany); see [34] for detailed information and properties of the oils. The dynamic viscosity η of each oil was measured using a common plate-to-plate setup as a function of temperature at a shear rate of $\dot{\gamma} = 100 \, \text{s}^{-1}$. Table 1 provides the viscosity classes and dynamic viscosities η of the oils.

Table 1. Viscosity classes (ISO VG) and dynamic viscosities $\eta(\vartheta)$ at different temperatures ϑ for the mineral oils used in this study.

Oil	Viscosity Class	Dynamic Viscosity $\eta(\vartheta)$ /mPas		
		η (20 °C)	η (25 °C)	η (30 °C)
FVA1	ISO VG 15	28	22	18
FVA2	ISO VG 32	72	54	42
FVA2 + FVA3	ISO VG 68	161	119	90
FVA3	ISO VG 100	288	205	150
FVA4	ISO VG 460	1543	1040	720

2.1.3. Hydraulic Rod

A hard-chrome plated hydraulic rod with a diameter $d = 50$ mm was used for the experiments. The rod was polished, since a mirror-smooth surface with good reflectivity was required for the film thickness measurements using ellipsometry. The same rod was already used in a previous study for film thickness measurements and has a roughness of R_z 0.1 μm and R_a 0.01 μm; see [29].

2.2. Ellipsometer Used for Film Thickness Meausrements

An ellipsometer is a highly accurate measurement device for the analysis of thin films in the nanometer range. A Plasmos SD 2000 ellipsometer was used for film thickness measurements on hydraulic rods. The same ellipsometer was already used in previous studies; see [29,30].

2.3. Test Rigs for Hydraulic Rod Seals

The friction of the rod seals was measured with two different test rigs at various operating conditions.

2.3.1. Common Test Rig for Friction Measurement on Two Seals

Figure 3 shows a schematic of the test rig used for friction measurements. The test rig is similar to a test arrangement, which is described in ISO 7986 [25] and used for the standardized analysis of friction of rod seals. It was also an arrangement in numerous scientific studies, e.g., [28,35–37].
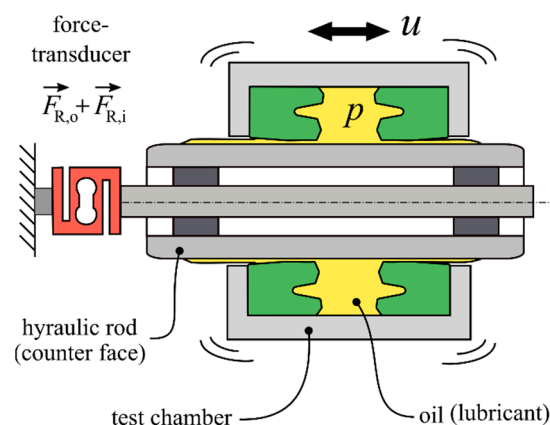
Figure 3. Schematic of the common test rig for friction measurements on two seals.

The sealing rings (e.g., U-cups) are installed in their housings in the manner prescribed by the seal manufacturer. Two housings each with one test seal ring are installed in a test chamber. In this arrangement, a linear drive cylinder is used to reciprocate the test chamber. The test chamber contains both seal rings, is filled with oil and pressurized using a separate hydraulic pump.

The resulting friction between the rod and both seal rings was measured using a force transducer. It should be noted that the measured friction

$$F_R = F_{R,o} + F_{R,i} \tag{2}$$

is always the sum of the friction from one seal at outstroke ($F_{R,o}$) and one seal at instroke ($F_{R,i}$).

2.3.2. New Test Rig

Figure 4 shows a schematic of the test rig developed and built for the novel measurement procedure described in Section 2.4. The aim was to keep the test rig design as simple as possible to guarantee easy handling of the components. We designed the new test rig without an oil chamber so that the rod and the seal ring can be removed from the test rig without any effort.

Figure 4. Schematic of the new test rig for friction measurements.

Using this test rig, the outstroke or instroke can be simulated with various rod speeds. The relative speed between the rod and the seal ring is realized by a linear drive unit (servo motor and ball screw unit) which pushes the seal housing in the axial direction with defined speed. Speeds in the range from 1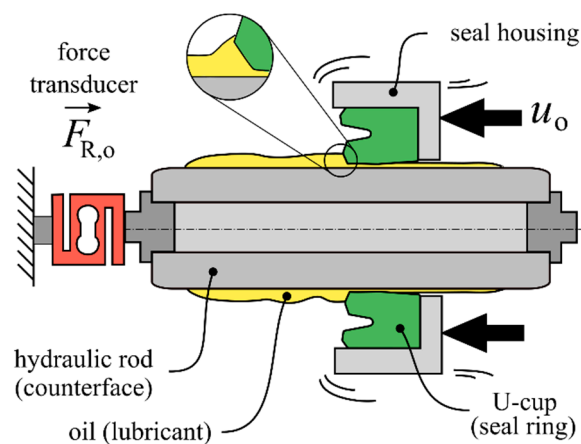 to 250 mms^{-1} are possible. An outstroke or instroke can only be performed at ambient pressure p_0. A force transducer is used to measure the resulting friction between the rod and the seal ring. Due to the radial load of the seal a concentric alignment between the rod and the seal is ensured.

2.4. Novel Measurement Procedure

Figure 5 illustrates the two main steps of the novel measurement procedure to analyze the friction of a rod seal at outstroke with predefined lubrication conditions and a certain fluid shear

$$\dot{\gamma} = u_{o,2}/h^*_{o,2} \tag{3}$$

in the sealing gap.

In the first step ①, a hydraulic rod with a certain oil film thickness $h_{o,1}$ is generated. Therefore, a proper amount of oil is wiped onto the rod. Then, oil on the rod is wiped off at a first outstroke using a seal ring and a defined stroke speed $u_{o,1}$. A thin oil film remains on the rod. Next, the seal ring is dismantled from the rod without touching the oil film. The remaining oil film thickness on the rod $h_{o,1}$ after this first outstroke is measured with the ellipsometer in circumferential and axial direction. Details on the film thickness measurement procedure can be found in [29,30]. After the film thickness measurement, a rod with a certain oil film thickness $h_{o,1}$ has been prepared. The film thickness $h_{o,1}$ depends on the rod speed $u_{o,1}$ and viscosity of oil η; see [29].

In the second step ②, a second outstroke is carried out on the same rod (without an instroke). Therefore, the seal ring is mounted and pushed again over the rod with an

increased speed $u_{o,2} > u_{o,1}$. Since the film thickness on the rod before the second outstroke $h_{o,1}$ is limited by the first outstroke with reduced rod speed $u_{o,1}$, the oil supply and film thickness in the sealing gap $h^*_{o,2}$ at the second outstroke are limited as well. Thus, the second outstroke is carried out at starved lubrication conditions. After the second outstroke, the film thickness on the rod $h_{o,2}$ is measured again. In Section 3.2.1, we show that the seal ring does not wipe off further oil at the second outstroke due to the increased speed.
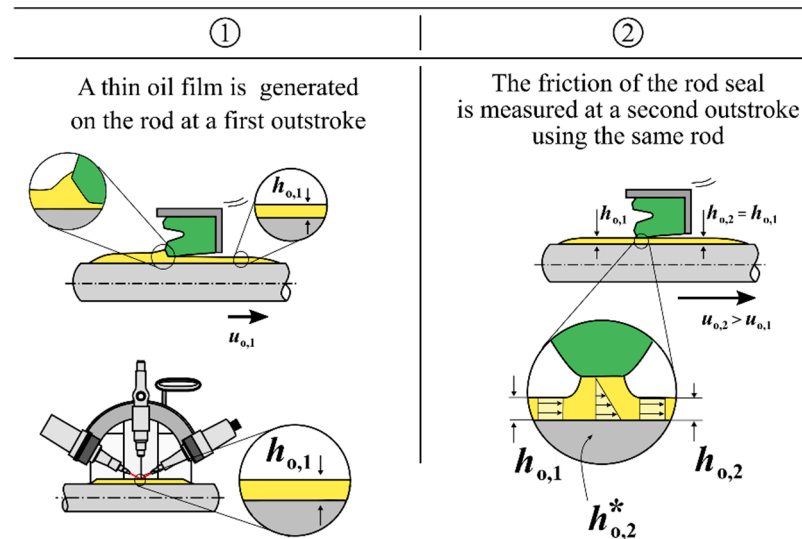

Figure 5. Illustration of step ① and step ② of the new measurement procedure.

When no further oil is wiped off from the rod at the second outstroke, the film thicknesses after both outstrokes are equal ($h_{o,1} = h_{o,2}$). Then, conclusions on the film thickness $h^*_{o,2}$ in the sealing gap at the second outstroke can be drawn. When Newtonian fluid behavior, the no-slip boundary condition, and a linear shear flow in the sealing gap are assumed, the film thickness in the sealing gap

$$h^*_{o,2} = 2 \, h_{o,2} \tag{4}$$

is twice the film thickness $h_{o,2}$ on the rod after both outstrokes. Since the film thickness on the rod $h_{o,2}$ is measured using ellipsometry and the rod speed $u_{o,2}$ is controlled by the test rig, the shear rate in the sealing gap $\dot{\gamma}$ can be determined. In conclusion, a predefined shear rate in the sealing gap at the second outstroke can be obtained by a certain outstroke speed $u_{o,2}$ and a proper limitation of the oil supply $h_{o,1}(u_{o,1}, \eta)$ through the first outstroke.

The Newtonian fluid friction

$$F_{\text{fluid}} = \dot{\gamma} \; \eta \; A = \frac{u_{o,2}}{2 \, h_{o,2}} \; \eta \, l_b \, d \, \pi \tag{5}$$

can be calculated based on the determined rod speed $u_{o,2}$, film thickness $h_{o,2}$, viscosity η, diameter of the rod d, and contact width l_b when using Equations (1), (3), and (4). It should be noted that numerical simulations of rod seals with U-cups revealed an approximately constant film thickness distribution in the sealing gap [26,38]. In addition, the apparent friction $F_{R,o,2}$ at the second outstroke is measured with the force transducer of the test rig; see Figure 4.

To sum up, the novel measurement procedure can be used to generate predefined shear rates in the sealing gap. Moreover, the apparent friction $F_{R,o,2}$ at outstroke can be analyzed in dependence of the fluid friction F_{fluid}; the latter is a function of the film thickness in the sealing gap, the rod speed, the contact area, and the dynamic viscosity of the lubricant.

3. Results

An empirical study on the friction of three different U-cups was carried out using the common method and the novel measurement procedure. We used mineral oils with different viscosities and a polished rod. All measurements were carried out at room temperature.

3.1. Common Test Method

The friction of three different rod seals was measured at various rod speeds u in the range of 10 to 500 mms^{-1}. All measurements were carried out at an operating pressure $p = 5$ bar. The surface temperature of the rod $\vartheta \approx 25\,^{\circ}$C was checked during the tests with a contact thermometer.

3.1.1. Measured Friction

Figure 6 shows the measured friction $F_R = F_{R,o} + F_{R,i}$ of the T20 U-cups in combination with different oils as a function of the rod speed. The friction of those seals depends on the rod speed u and the viscosity η of the oil in the test chamber. When using oils with a lower viscosity, the friction at low rod speeds was higher. In contrast, oils with a lower viscosity resulted in lower friction at higher rod speeds. Further measurements with similar results were carried out using the EW U-cups. The results are listed in Table A1 in Appendix A.
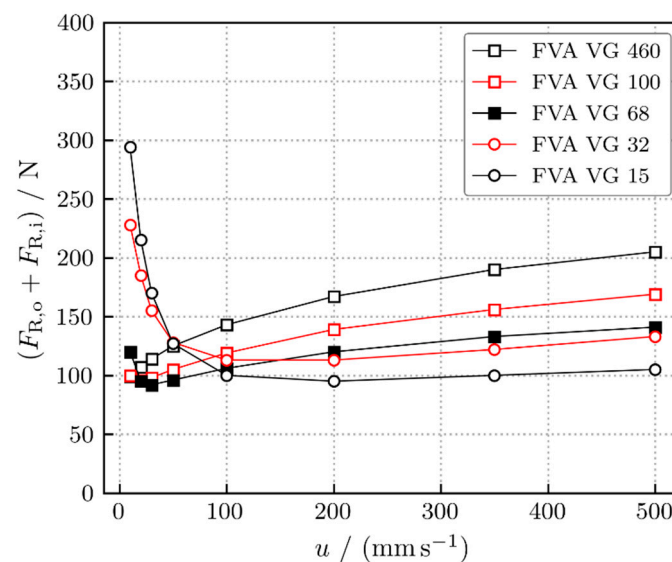
Figure 6. Measured friction of two seals as a function of rod speed; the results were obtained using the common method ($u = 10 \ldots 500$ mms^{-1}, $\vartheta = 25\,^{\circ}$C, $p = 5$ bar, various mineral oils, T20 U-cups).

3.1.2. Measured Friction vs. Hydrodynamic Parameter

The measured friction in the previous section can be illustrated using a hydrodynamic parameter

$$G_{\text{hyd}} = u\,\eta \tag{6}$$

which is defined as the product of rod speed and viscosity. This hydrodynamic parameter is a simplification of the so-called 'Stribeck', 'Hersey', or 'Gümbel' number. Figure 7 shows the measured friction of the three different rod seals as a function of the hydrodynamic parameter G_{hyd}. Due to the introduction of the hydrodynamic parameter G_{hyd}, the friction of each seal can be approximated for a wide range of rod speeds and viscosities in a single reference curve. The shapes of the friction curves for the different seal rings are similar. As shown in Figure 7, the friction of both EW U-cups is lower than the friction of the T20 U-cups for the chosen operating conditions.
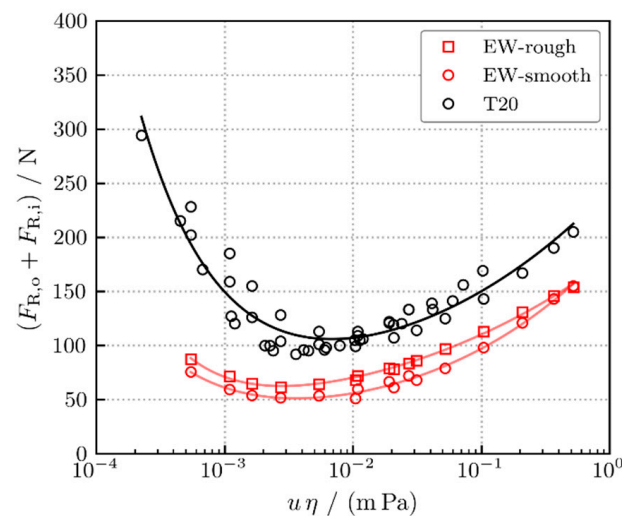
Figure 7. Measured friction of two seals as a function of the hydrodynamic parameter G_{hyd}; the results were obtained using the common method ($u = 10 \ldots 500 \, \text{mms}^{-1}$, $\vartheta = 25 \, °C$, $p = 5 \, \text{bar}$, various mineral oils, T20 and EW U-cups).

3.2. New Procedure

The ratio $u_{o,1}/u_{o,2}$ of the rod speeds at first and second outstroke was varied to achieve various film thicknesses and shear rates in the sealing gap. All measurements were carried out at ambient pressure $p = p_0$. A complete list of the measured values can be found in Tables A2 and A3 in Appendix A.

3.2.1. Measured Friction and Film Thickness

In this section, a representative selection of the measurement results is shown for illustration purposes. Figure 8a shows the measured friction $F_{R,o,1}$ at a first outstroke and $F_{R,o,2}$ at the second outstroke on the same rod using the new procedure. We used the mineral oil FVA 4 (ISO VG 460) and a T20 U-cup. The rod speed at the first outstroke $u_{o,1} = 10 \, \text{mms}^{-1}$ was constant, whereas the rod speed at the second outstroke $u_{o,2}$ was increased stepwise. For each speed ratio $u_{o,1}/u_{o,2}$, the procedure was repeated three times. The measured friction $F_{R,o,1}$ at the first outstroke was almost constant. However, the friction $F_{R,o,2}$ at the second outstroke at an increased rod speed $u_{o,2}$ increased from approximately 60 N to 270 N. Figure 8b shows the corresponding film thickness after the first and second outstroke as well. The film thickness after the second outstroke $h_{o,2}$ was almost equal the film thickness $h_{o,1}$ after the first outstroke. Differences are only in the range of a few nanometers.

To sum up, if the film thickness $h_{o,1}$ and $h_{o,2}$ on the rod before and after the second outstroke were constant. The friction $F_{R,o,2}$ at the second outstroke depended on rod speed $u_{o,2}$ due to the increased shear rate in the sealing gap, which resulted from an increased speed $u_{o,2}$ and limited film thickness $h_{o,1}$.

For the results in Figure 9, we used mineral oil FVA2 (ISO VG 32) and a T20 U-cup. Both the rod speed at the first outstroke $u_{o,1}$ and at the second outstroke $u_{o,2}$ were increased. The ratio $u_{o,1}/u_{o,2}$ of the rod speeds was constant. Differences related to the friction, Figure 9a, were less significant compared to the results shown in Figure 8a. Figure 9b shows the results of the corresponding film thickness measurements. The film thickness $h_{o,1}$ after the first outstroke increased with the rod speed $u_{o,1}$ as expected; see [26,29]. The film thickness $h_{o,2}$ after the second outstroke was almost equal to the film thickness $h_{o,1}$ after the first outstroke. Differences are only in the range of a few nanometers.

To sum up, the film thickness measurements using ellipsometry on the rod after both outstrokes prove that differences related to the film thickness are pretty small. It is assumed that no further oil was wiped off the rod at the second outstroke with an increased rod speed. The measured film thickness depends on the rod speed at the first outstroke and

the viscosity of the oil, but not on the rod speed at the second outstroke. For further discussion on the oil film generation of those seals, refer to [26,29]. Moreover, results in Figures 8 and 9 indicate that the friction at the second outstroke $F_{R,o,2}$ strongly depends on the film thickness $h_{o,1}$ on the rod after the first outstroke and the rod speed $u_{o,2}$ at the second outstroke. As discussed in Section 2.4, the shear rate in the sealing gap is in direct correlation with $h_{o,1}$ and $u_{o,2}$.

(a)   (b)
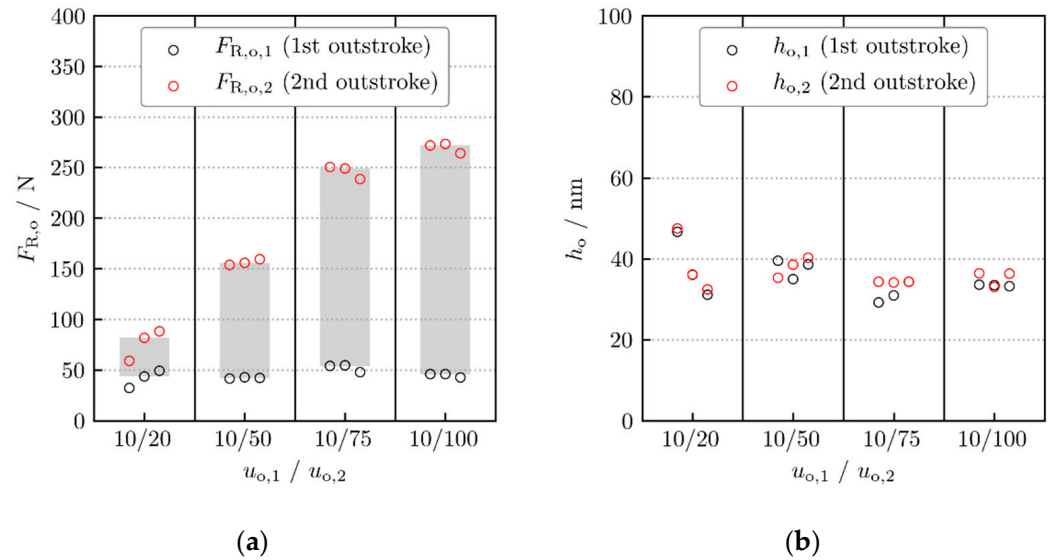
Figure 8. Measured friction (**a**) and film thickness (**b**) at first and second outstroke using the new method with constant speed at first outstroke $u_{o,1} = 10\,\mathrm{mms^{-1}}$ (room temperature, ambient pressure, ISO VG 460 mineral oil with $\eta(23\,^{\circ}\mathrm{C}) = 1214\,\mathrm{mPas}$, T20 U-cups).

(a)   (b)
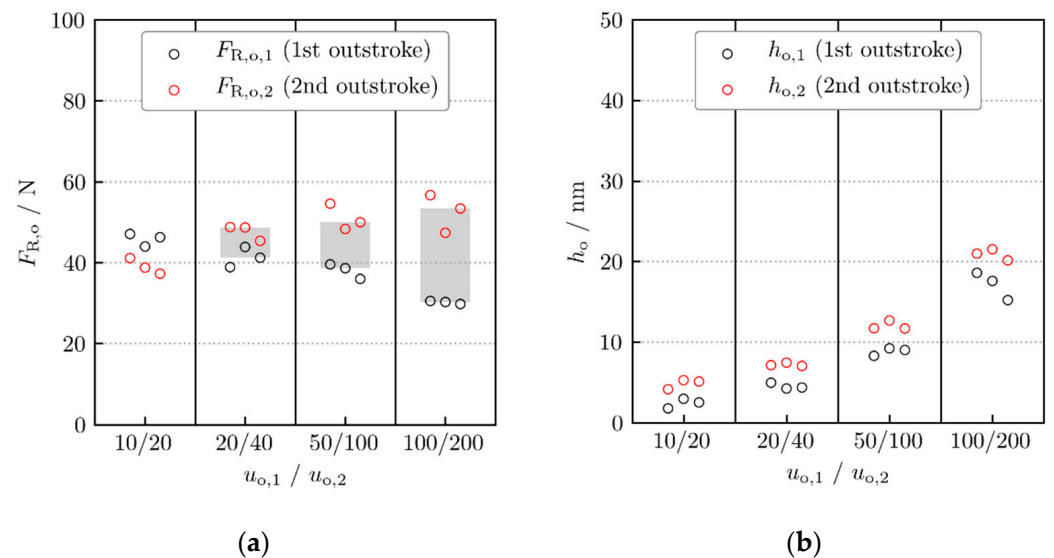
Figure 9. Measured friction (**a**) and film thickness (**b**) at first and second outstroke using the new method with constant speed ratios $u_{o,1}/u_{o,2} = 0,5$ (room temperature, ambient pressure, ISO VG 32 mineral oil with $\eta(23\,^{\circ}\mathrm{C}) = 60\,\mathrm{mPas}$, T20 U-cups).

3.2.2. Measured Friction vs. Calculated Fluid Friction

In this section, the focus is on the friction $F_{R,o,2}$ at the second outstroke, which depends on $h_{o,1}$ and $u_{o,2}$. Each second outstroke was carried out with a limited and measured oil film thickness $h_{o,1}$, as described in Section 2.4 and shown by empirical results in Section 3.2.1. In accordance with Equation (5), the fluid friction $F_{R,o,2}$ at the second outstroke was calculated

using the film thickness $h_{o,2}$, the rod speed $u_{o,2}$, the dynamic viscosity η of the oil, and the contact area A as inputs.

Figure 10 shows the measured friction $F_{R,o,2}$ at the second outstroke plotted against the calculated fluid friction F_{Fluid} according to Equation (5). The fluid friction is calculated using the following measured parameters: the dynamic viscosity of the oil, the rod speed, the film thickness and the contact area between the U-cups and the rod.

Figure 10. The measured friction at the second outstroke with predefined lubrication conditions is plotted against the calculated fluid friction based on the measurement results obtained with the new procedure (room temperature, ambient pressure, mineral oils, T20 and EW U-cups).

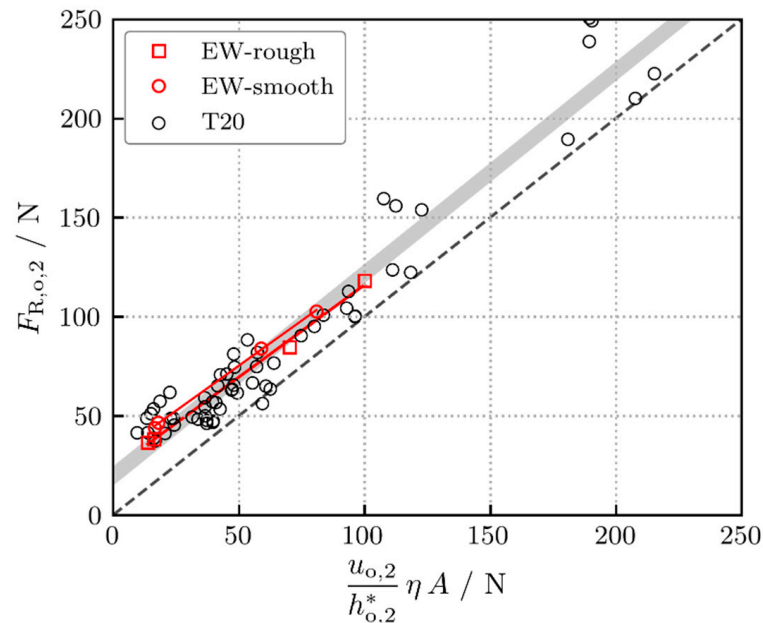A linear correlation between the measured friction and the calculated fluid friction exists. The measured friction was approximately 20 N higher than the calculated friction based on the assumption of pure fluid friction. However, the calculated fluid friction based on fundamental tribological parameters is a good approximation of the apparent and measured friction.

4. Discussion

We introduced a new measurement procedure for an advanced analysis of the friction of reciprocating rod seals. In an exemplary way, we used the new procedure (Section 2.4) and a common method (Section 2.3.1) to compare the friction of different rod seals.

4.1. New Measurement Procedure

The new measurement procedure is a combination of film thickness measurements and friction measurements. It is possible to analyze the friction of common rod seals at predefined lubrication conditions due to a limited oil supply. Therefore, a thin oil film in the nanometer range is deposited on the rod before outstroke.

Instead of measuring the gap height between the seal ring and the rod directly, the oil film thickness on the rod is measured before and after the outstroke. Assuming a linear shear flow and Newtonian fluid behavior, the film thickness in the gap can be calculated based on the film thickness on the rod; see Section 2.4. The friction force of the rod seal that actually occurs during the outstroke is measured using the test rig.

For the film thickness measurements, we used ellipsometry to guarantee a high accuracy in the nanometer range; see [26,29,30] for examples. Alternative methods for film thickness measurements require hollow and transparent glass rods [39–42], modified sealing rings [43,44], or modified lubricants [45]. One main advantage is that we can use

almost any hydraulic rod made of different materials, e.g., hard-chromed rods as it is state of the art for hydraulic and pneumatic rods. The only restriction is that the surface of the rod must be polished since a certain reflectivity is required for the analysis with the ellipsometer. Furthermore, seal rings with a different profile, nominal diameter, surface roughness, and made of different materials can be analyzed. It is not necessary to modify the seal rings before the analysis. Here, we used mineral oils with different viscosities. However, ellipsometry and the procedure is not limited to mineral oils. Further oils and lubricants with various chemical properties and based on different base oils (e.g., silicone oil [46]) can be analyzed without additional experimental effort.

By separating film thickness measurements and friction measurements, the operating parameters are only limited by the test rig used. For further operating conditions, such as increased operating pressures, speeds, or a certain temperature, the test rig can be modified. However, for a comparison of different seal rings or lubricants, the test rig shown is suitable.

Based on results from an empirical study, the measured friction of different rod seals was approximated as a function of the calculated fluid friction with good agreement. The difference between the calculated fluid friction and the measured friction was constant and approximately 20 N. The fluid friction was determined based on the following measured tribological parameters: the film thickness in the sealing gap, the rod speed, the dynamic viscosity of the oil, and the contact area between the seal ring and the rod. It is conceivable that differences between the measured and calculated friction result from the assumption of pure Newtonian friction and neglecting boundary friction. Results in Figures 6 and 7 indicate an increase in boundary friction for low viscous oil at low speeds ($G_{\mathrm{hyd}} < 2 \times 10^{-3}$ m Pa). This is probably the result of very thin lubrication films that are only in the low single-digit nanometer range for such seals; see [26,29]. Since the measured friction forces in Figure 10 are slightly higher than the calculated friction force, the presence of boundary friction and the assumption of a mixed lubrication regime seems to be confirmed. In general, the results shown in this study are plausible and reproducible.

This procedure can be used for the comparison of the resulting friction force of different sealing rings and to analyze mechanisms in thin films in a more general way. The empirical results from our first empirical study demonstrate that it is possible to control the shear rate in a range of approximately 10^5 to 10^7 s^{-1} and the gap height in a range of approximately 5 to 100 nm. In such narrow gaps and at such high shear rates, tribological phenomena such as wall slip, shear thinning, or an increase in the lubricant's viscosity were observed by other authors; see Section 1. Those phenomena depend on the film thickness, shear rate, and intermolecular forces between the lubricant and the surfaces. Besides the film thickness and the shear rate, the new measurement procedure can be used to analyze the influence of intermolecular forces and interfacial phenomena in the sealing gap on the resulting friction. In a next step, lubricants with different additives and made from different base oils can be compared at various shear rates and gap heights. Furthermore, the materials of the rod and the sealing ring can be varied. Using the new procedure, it is now possible to analyze whether and to what extend certain tribological phenomena influence the friction of rod seals. It can be clarified as to which phenomena should be considered when modelling linear reciprocating contacts.

4.2. On the Analyis of Friction of Rod Seals

The friction of the three different seal rings was compared using the common method and the novel measurement procedure. Depending on the question asked, the results from both approaches have their advantages.

If a proper sealing ring must be chosen for certain operating parameters, the common and standardized method according to ISO 7986 [25] is very helpful. The friction of various sealing rings can be measured at various operating parameters. The seal ring resulting in the lowest friction should be recommended. However, the method does not provide any information on the lubrication conditions that are a key factor influencing the friction.

Thus, an in-depth analysis of friction mechanisms in the sealing gap is not possible. If the causes of the frictional behavior are not of great interest, the standardized method is a good choice.

For a more in-depth analysis of the friction of rod seals, we recommend the use of the new procedure. In an exemplary way, the friction of seal rings which differ in their geometry and surface topography was compared. Despite their differing properties, it was possible to approximate the apparent friction of those seals by the calculated Newtonian fluid friction based on the measured film thickness, speed, viscosity, and contact area. Consequently, the influence of the seal ring's surface topography on the shear flow in the sealing gap and the friction was small in this specific example.

However, when further tribological mechanisms have a significant influence on friction, discrepancies between Newtonian fluid friction and apparent friction can be indicated by the new procedure. When only using the standardized method without measuring the film thickness and shear rate, such phenomena cannot be identified with certainty. With the new procedure, the expected fluid friction can be determined based on measured values and compared to occurring friction forces. Consequently, an advanced discussion on mechanisms in the sealing gap of rod seals is now possible.

5. Conclusions

A new perspective on thin film lubrication and the friction of common rod seals is provided by the empirical analysis of predefined lubrication conditions and shear rates. The originality of the new measurement procedure comes from the fact that the apparent friction of seal rings (e.g., polyurethane U-cup rod seals) with various geometries, surface topographies, and other properties can be analyzed as a function of fundamental tribological parameters, such as film thickness, rod speed, contact area, and viscosity. It is remarkable that the film thickness in the sealing gap can be predefined in the nanometer range. Furthermore, shear rates in the range of 10^5 to 10^7 s^{-1} can be controlled. In other words, rod seals can be utilized as an oil film generator and as part of a thin film tribometer for linear contacts.

The friction of the analyzed sealing systems was dominated by Newtonian fluid friction, even at high shear rates and thin film lubrication conditions in the nanometer range. It was possible to compare the friction of three different U-cups with different geometry and surface roughness in direct relation to the viscosity of the oil, the shear rate, and the contact area between the rod and the seal ring.

In general, the novel measurement procedure is useful when comparing the frictional behavior of rod seals with different properties. In the development process of seal rings, the procedure can be adopted for optimizing the geometry, surface topography, and the resulting lubrication conditions. Moreover, lubricants based on various base oils and additives can be analyzed in a similar way to draw conclusions on their tribological properties in such narrow gaps and at high shear rates. The results obtained using the new procedure are useful for the validation of modern simulation models for the oil film generation and friction of reciprocating rod seals.

When using a common method similar to the one described in ISO 7986 [25] for analyzing the friction of rod seals, we suggest to show the friction of rod seals as a function of the hydrodynamic parameter G_{hyd}, which includes the rod speed and dynamic viscosity of the oil. Then, the friction of a rod seal can be described as a reference curve for a wide range of operating parameters, including various rod speeds and viscosities. Such a reference curve is useful for the comparison of different rod seals at certain operating parameters and can be used for further discussion.

Nomenclature

A	Contact area between a seal ring and a rod
d	Nominal diameter of a rod
F_{fluid}	Newtonian fluid friction
F_{R}	Measured friction at the test rig for two seals
$F_{\text{R,i}}$	Friction of one rod seal at instroke
$F_{\text{R,o}}$	Friction of one rod seal at outstroke
G_{hyd}	Hydrodynamic parameter
$h_{\text{o,1}}$	Film thickness on the rod after the 1st outstroke when using the new procedure
$h_{\text{o,2}}$	Film thickness on the rod after the 2nd outstroke when using the new procedure
l_{b}	Contact width between the seal ring and the rod, measured in axial direction
p_0	Ambient pressure
p	Operating pressure
u_{o}	Rod speed at outstroke
$u_{\text{o,1}}$	Rod speed at 1st outstroke when using the new procedure
$u_{\text{o,2}}$	Rod speed at 2nd outstroke when using the new procedure
$\dot{\gamma}$	Shear rate
η	Dynamic viscosity
ϑ	Temperature

Appendix A

Table A1. Measured friction of two rod seals using the common method.

U-Cup	Oil	$\frac{\eta\,(25\,^\circ\text{C})}{\text{mPas}}$	Rod Speed u in mms^{-1}							
			10	20	30	50	100	200	350	500
			Friction Force $F_R(u)$ in N							
T20	FVA1	22	294	215	170	127	100	95	100	105
T20	FVA2	54	228	185	155	128	113	113	122	133
T20	FVA2	54	202	159	126	104	101	109	121	134
T20	FVA3	205	100	96	98	105	119	139	157	169
T20	FVA4	1040	99	107	114	125	143	167	190	205
T20	ISO VG 68	119	120	95	92	96	107	121	133	141
EW-rough	FVA2	54	87	71	65	61	64	72	79	84
EW-rough	FVA4	1040	68	78	86	97	113	131	146	154
EW-smooth	FVA2	54	75	59	54	52	54	60	67	72
EW-smooth	FVA4	1040	51	61	68	79	98	121	143	156

Table A2. Measured friction and film thickness of rod seals at outstroke using the new measurement procedure and T20 U-cups at room temperature.

U-Cup	Oil	$\frac{\eta\ (23\ °C)}{mPas}$	$\frac{u_{o,2}}{mms^{-1}}$	$\frac{h_{o,2}}{nm}$	$\frac{F_{R,o,2}}{N}$	U-Cup	Oil	$\frac{\eta\ (23\ °C)}{mPas}$	$\frac{u_{o,2}}{mms^{-1}}$	$\frac{h_{o,2}}{nm}$	$\frac{F_{R,o,2}}{N}$
T20	FVA1	24	10	0.4	70.7	T20	FVA3	234	40	14.8	71.1
T20	FVA1	24	10	0.8	61.8	T20	FVA3	234	100	7.8	222.5
T20	FVA1	24	10	0.9	57.3	T20	FVA3	234	100	8.0	210
T20	FVA1	24	20	1.1	49.4	T20	FVA3	234	100	9.2	189.4
T20	FVA1	24	20	2.5	41.5	T20	FVA3	234	100	29.3	74.8
T20	FVA1	24	20	3.6	41.4	T20	FVA3	234	100	33.8	61.6
T20	FVA1	24	40	4.3	53.5	T20	FVA3	234	100	35.2	63.4
T20	FVA1	24	40	4.6	51.1	T20	FVA3	234	200	28.2	122.3
T20	FVA1	24	40	5.1	48.8	T20	FVA3	234	200	30.1	123.6
T20	FVA2	60	20	4.1	41.2	T20	FVA3	234	200	34.7	100.3
T20	FVA2	60	20	5.1	37.3	T20	FVA3	234	200	34.7	100.0
T20	FVA2	60	20	5.3	38.8	T20	FVA3	234	200	35.7	112.7
T20	FVA2	60	40	7.0	45.4	T20	FVA3	234	200	36.0	104.3
T20	FVA2	60	40	7.1	48.8	T20	FVA3	234	200	55.0	65.0
T20	FVA2	60	40	7.5	48.7	T20	FVA3	234	200	60.3	66.6
T20	FVA2	60	100	11.7	50.0	T20	FVA3	234	200	70.9	63.0
T20	FVA2	60	100	11.7	54.6	T20	FVA4	1214	20	32.4	88.3
T20	FVA2	60	100	12.7	48.3	T20	FVA4	1214	20	36.1	81.2
T20	FVA2	60	200	10.2	100.8	T20	FVA4	1214	20	47.5	59.1
T20	FVA2	60	200	10.7	95.1	T20	FVA4	1214	50	35.3	153.8
T20	FVA2	60	200	11.5	90.4	T20	FVA4	1214	50	38.5	155.8
T20	FVA2	60	200	20.1	53.4	T20	FVA4	1214	50	40.3	159.5
T20	FVA2	60	200	21.0	56.7	T20	FVA4	1214	75	34.1	249.2
T20	FVA2	60	200	21.5	47.4	T20	FVA4	1214	75	34.3	238.7
T20	FVA3	234	10	2.7	63.5	T20	FVA4	1214	75	34.3	250.6
T20	FVA3	234	10	2.8	56.2	T20	FVA4	1214	100	33.1	273.4
T20	FVA3	234	10	3.5	74.6	T20	FVA4	1214	100	36.3	264.2
T20	FVA3	234	20	7.0	65.5	T20	FVA4	1214	100	36.4	271.9
T20	FVA3	234	20	8.0	65.2	T20	FVA4	1214	100	218.4	46.7
T20	FVA3	234	20	8.4	57.1	T20	FVA4	1214	100	232.6	47.7
T20	FVA3	234	40	10.5	76.6	T20	FVA4	1214	100	232.6	46.2
T20	FVA3	234	40	11.6	81.9						

Table A3. Measured friction and film thickness of rod seals at outstroke using the new measurement procedure and EW U-cups.

U-Cup	Oil	$\frac{\eta\ (23\ °C)}{mPas}$	$\frac{u_{o,2}}{mms^{-1}}$	$\frac{h_{o,2}}{nm}$	$\frac{F_{R,o,2}}{N}$	U-Cup	Oil	$\frac{\eta\ (23\ °C)}{mPas}$	$\frac{u_{o,2}}{mms^{-1}}$	$\frac{h_{o,2}}{nm}$	$\frac{F_{R,o,2}}{N}$
	FVA2	60	80	12.0	46.7		FVA2	60	80	13.3	38.4
EW-smooth	FVA2	60	80	13.0	44.0	EW-rough	FVA2	60	80	15.6	36.6
	FVA3	234	75	9.7	102.8		FVA3	234	75	7.8	118.4
	FVA3	234	75	13.4	84.0		FVA3	234	75	11.2	84.8

References

1. Müller, H.K.; Nau, B.S. *Fluid Sealing Technology: Principles and Applications*; Marcel Dekker: New York, NY, USA, 1998; ISBN 0-8247-9969-0.
2. Bauer, F. *Tribologie—Prägnant Und Praxisrelevant*; Springer Vieweg: Wiesbaden, Germany, 2021; ISBN 978-3-658-32920-4.
3. Flitney, R. Reciprocating Seals. In *Seals and Sealing Handbook*; Butterworth-Heinemann: Oxford, UK, 2014; pp. 289–367, ISBN 978-0-08-099416-1.
4. Gee, M.L.; McGuiggan, P.M.; Israelachvili, J.N.; Homola, A.M. Liquid to Solidlike Transitions of Molecularly Thin Films under Shear. *J. Chem. Phys.* **1990**, *93*, 1895–1906. [CrossRef]
5. Shen, M.; Luo, J.; Wen, S. Effects of Surface Physicochemical Properties on the Tribological Properties of Liquid Paraffin Film in the Nanoscale. *Surf. Interface Anal.* **2001**, *32*, 286–288. [CrossRef]
6. Luo, J.; Wen, S.; Xuanyu, S. Substrate Surface Energy Effects on a Liquid Lubricant Film at Nanometre Scale. *Lubr. Sci.* **1998**, *11*, 936–1198.

7. Neto, C.; Evans, D.R.; Bonaccurso, E.; Butt, H.-J.; Craig, V.S.J. Boundary Slip in Newtonian Liquids: A Review of Experimental Studies. *Rep. Prog. Phys.* **2005**, *68*, 2859–2897. [CrossRef]
8. Lauga, E.; Brenner, M.; Stone, H. Microfluidics: The No-Slip Boundary Condition. In *Springer Handbook of Experimental Fluid Mechanics*; Springer: Berlin/Heidelberg, Germany, 2007; pp. 1219–1235. ISBN 978-3-540-30299-5.
9. Lee, T.; Charrault, E.; Neto, C. Interfacial Slip on Rough, Patterned and Soft Surfaces: A Review of Experiments and Simulations. *Adv. Colloid Interface Sci.* **2014**, *210*, 21–38. [CrossRef]
10. Spikes, H.A. Slip at the Wall—Evidence and Tribological Implications. *Tribol. Ser.* **2003**, *41*, 525–535. [CrossRef]
11. Spikes, H. Friction Modifier Additives. *Tribol. Lett.* **2015**, *60*, 5. [CrossRef]
12. Porter, R.S.; Johnson, J.F. Viscosity Performance of Lubricating Base Oils at Shears Developed in Machine Elements. *Wear* **1961**, *4*, 32–40. [CrossRef]
13. Panwar, P.; Michael, P.; Devlin, M.; Martini, A. Critical Shear Rate of Polymer-Enhanced Hydraulic Fluids. *Lubricants* **2020**, *8*, 102. [CrossRef]
14. Bair, S.; Qureshi, F. The Generalized Newtonian Fluid Model and Elastohydrodynamic Film Thickness. *J. Tribol.* **2003**, *125*, 70–75. [CrossRef]
15. Wang, J.; Li, Y.; Lian, Z. Numerical Investigations on the Sealing Performance of a Reciprocating Seal Based on the Inverse Lubrication Method. *J. Tribol.* **2019**, *141*, 112201. [CrossRef]
16. Kaiser, F. Ein Simulationsmodell zur Analyse des Schmierfilms von Stangendichtungen. Ph.D. Thesis, TU Kaiserslautern, Kaiserslautern, Germany, 2015.
17. Crudu, M.; Fatu, A.; Cananau, S.; Hajjam, M.; Pascu, A.; Cristescu, C. A Numerical and Experimental Friction Analysis of Reciprocating Hydraulic "U" Rod Seals. *Proc. Inst. Mech. Eng. Part J J. Eng. Tribol.* **2012**, *226*, 785–794. [CrossRef]
18. Fatu, A.; Hajjam, M. Numerical Modelling of Hydraulic Seals by Inverse Lubrication Theory. *Proc. Inst. Mech. Eng. Part J J. Eng. Tribol.* **2011**, *225*, 1159–1173. [CrossRef]
19. El Gadari, M.; Hajjam, M. Effect of the Grooved Rod on the Friction Force of U-Cup Hydraulic Rod Seal with Rough Lip. *Tribol. Trans.* **2018**, *61*, 661–670. [CrossRef]
20. Huang, P. *Numerical Calculation of Elastohydrodynamic Lubrication*; Wiley-VCH: Singapore, 2015; ISBN 978-1-118-92096-1.
21. Stupkiewicz, S.; Marciniszyn, A. Elastohydrodynamic Lubrication and Finite Configuration Changes in Reciprocating Elastomeric Seals. *Tribol. Int.* **2009**, *42*, 615–627. [CrossRef]
22. Spikes, H.; Jie, Z. History, Origins and Prediction of Elastohydrodynamic Friction. *Tribol. Lett.* **2014**, *56*, 1–25. [CrossRef]
23. Huang, Y.; Salant, R.F. Simulation of a Hydraulic Rod Seal with a Textured Rod and Starvation. *Tribol. Int.* **2016**, *95*, 306–315. [CrossRef]
24. Gropp, A. Simulation of Surface Topography in Sealing Systems for Reciprocating Rods. In Proceedings of the 19th International Sealing Conference, Stuttgart, Germany, 12–13 October 2016; VDMA Fluidtechnik: Stuttgart, Germany, 2016; pp. 193–203.
25. *ISO 7986:1997-07*; Hydraulic Fluid Power—Sealing Devices—Standard Test Methods to Assess the Performance of Seals Used in Oil Hydraulic Reciprocating Applications. Beuth Verlag GmbH: Berlin, Germany, 1997.
26. Feuchtmüller, O.; Dakov, N.; Hörl, L.; Bauer, F. Remarks on Modeling the Oil Film Generation of Rod Seals. *Lubricants* **2021**, *9*, 95. [CrossRef]
27. Nikas, G.K. Eighty Years of Research on Hydraulic Reciprocating Seals: Review of Tribological Studies and Related Topics since the 1930s. *Proc. Inst. Mech. Eng. Part J J. Eng. Tribol.* **2010**, *224*, 1–23. [CrossRef]
28. Visscher, M.; Kanters, A.F.C. Literature Review and Discussion on Measurements of Leakage, Lubricant Film Thickness and Friction of Reciprocating Elastomeric Seals. *Lubr. Eng.* **1990**, *46*, 785–791.
29. Feuchtmüller, O.; Hörl, L.; Bauer, F. Oil Film Generation of a Hydraulic Rod Seal: An Experimental Study Using Ellipsometry. *Tribol. Int.* **2021**, *162*, 107102. [CrossRef]
30. Hörl, L.; Haas, W.; Nißler, U. A Comparison of Test Methods for Hydraulic Rod Seals. *Seal. Technol.* **2009**, *2009*, 8–13. [CrossRef]
31. Feldmeth, S.; Stoll, M.; Bauer, F. How to Measure the Radial Load of Radial Lip Seals. In Proceedings of the 61. Tribologie-Fachtagung, Göttingen, Germany, 28–30 September 2020; pp. 5–12.
32. *DIN 3761-9*; Radial-Wellendichtringe für Kraftfahrzeuge, Prüfung Radialkraft-Meßgerät-Digital. Beuth Verlag GmbH: Berlin, Germany, 1984.
33. *SAE J1901:1988-06*; Recommended Practice: Lip Force Measurement—Radial Lips Seals. Society of Automotive Engineers: Warrendale, PA, USA, 1988; (Cancelled in 2002-10).
34. *FVA Heft 660*; Referenzölkatalog (Datensammlung). Forschungsvereiningung Antriebstechnik eV.: Frankfurt, Germany, 2007.
35. Lang, C.M. Untersuchungen an Berührungsdichtungen für Hydraulische Arbeitszylinder. Ph.D. Thesis, University of Stuttgart, Stuttgart, Germany, 1960.
36. Messner, N. Untersuchung von Hydraulik-Stangendichtungen aus Polytetrafluoräthylen. Ph.D. Thesis, Universität Stuttgart, Stuttgart, Germany, 1985.
37. Prokop, H.-J. Zum Abdicht-und Reibungsverhalten von Hydraulik-Stangendichtungen aus Polytetrafluoräthylen. Ph.D. Thesis, Universität Stuttgart, Stuttgart, Germany, 1989.
38. Salant, R.F.; Maser, N.; Yang, B. Numerical Model of a Reciprocating Hydraulic Rod Seal. *J. Tribol.* **2006**, *129*, 91–97. [CrossRef]

39.　Ottink, K.; Wennehorst, B.; Poll, G. Analysis of Rod Seals by Application of the Light Induced Fluorescence Method. In Proceedings of the 16th International Sealing Conference, Stuttgart, Germany, 12–13 October 2010; VDMA Fluidtechnik: Stuttgart, Germany, 2010; pp. 101–111.

40.　Goerres, M.; Murrenhoff, H. Schmierfilmdickenmessung Mit Hilfe Der Interferenz- Und Fluoreszenzmethode. In Proceedings of the 13th International Sealing Conference, Stuttgart, Germany, 5–6 October 2004; VDMA Fluidtechnik: Stuttgart, Germany, 2004; pp. 254–266.

41.　Fowell, M.T.; Myant, C.; Spikes, H.A.; Kadiric, A. A Study of Lubricant Film Thickness in Compliant Contacts of Elastomeric Seal Materials Using a Laser Induced Fluorescence Technique. *Tribol. Int.* **2014**, *80*, 76–89. [CrossRef]

42.　Yoshimura, K.; Suzuki, N.; Mizuta, H. Oil Film Formation of Reciprocating Seals Observed by Interferometry. *Tribol. Online* **2014**, *9*, 106–112. [CrossRef]

43.　Blok, H.; Koens, H.J. The Breathing Film between a Flexible Seal and a Reciprocating Rod. *Proc. Inst. Mech. Eng.* **1965**, *180*, 221–223. [CrossRef]

44.　Kaneta, M.; Todoroki, H.; Nishikawa, H.; Kanzaki, Y.; Kawahara, Y. Tribology of Flexible Seals for Reciprocating Motion. *J. Tribol.* **2000**, *122*, 787–795. [CrossRef]

45.　Suzuki, N.; Mizuta, H.; Sato, Y. An Experimental Approach to the Sealing Mechanism of the Reciprocating Seals. In Proceedings of the 17th International Sealing Conference, Stuttgart, Germany, 13–14 September 2012; VDMA Fluidtechnik: Stuttgart, Germany, 2012; pp. 483–490.

46.　Meyer, F.; Loyen, C.F. The Creep of Oil on Steel Followed by Ellipsometry. *Wear* **1975**, *33*, 317–323. [CrossRef]